New Journal of Physics
The open-access journal for physics

Coherent and incoherent radiation from a channel-guided laser wakefield accelerator

A G Khachatryan[1], **F A van Goor and K-J Boller**
Faculty of Science and Technology, MESA+ Institute, University of Twente, PO Box 217, 7500 AE Enschede, The Netherlands
E-mail: A.Khachatryan@tnw.utwente.nl

New Journal of Physics **10** (2008) 083043 (12pp)
Received 30 May 2008
Published 29 August 2008
Online at http://www.njp.org/
doi:10.1088/1367-2630/10/8/083043

Abstract. Coherent and incoherent electromagnetic radiation emitted from a channel-guided laser wakefield accelerator (LWFA) is calculated based on the Lienard–Wiechert potentials. It is found that at wavelengths longer than the bunch length, the radiation is coherent. The coherent radiation, which typically lies in the infrared range, shows features that reveal details of the acceleration process and properties of the electron bunch, such as its duration, charge, energy, and offset with respect to the wakefield axis. It is found that the LWFA emits energy predominantly in the coherent range of frequencies. The incoherent range of the spectrum, which extends to the x-ray frequency range, consists of rather broad peaks caused by the acceleration. The radiated energy, power and the pulse duration are estimated.

Contents

[1] Author to whom any correspondence should be addressed.

1. Introduction

Progress in charged particles physics usually leads to advances also in radiation physics (e.g. in new radiation sources). A well-known example of this is synchrotron radiation: a radio frequency (RF) electromagnetic wave accelerates electron bunches to relativistic energies; in turn, these bunches may generate the electromagnetic synchrotron radiation that has become a valuable tool for research and many applications. The laser wakefield accelerator (LWFA) is a new type of accelerator. In LWFA, a high-intensity laser pulse, with duration of the order of the plasma wave period, generates very strong accelerating and focusing fields (wakefield) in the plasma [1, 2]. Accelerating gradients as high as a few tens of GV m^{-1} have been measured in experiments [3], which is three orders of magnitude higher than what can be achieved in conventional RF accelerators. This makes LWFA very attractive for electron acceleration. Recently, extremely small, micron-sized relativistic electron-bunches were generated by laser wakefield acceleration in the so-called bubble regime [4]–[6], where some background plasma electrons are trapped and accelerated in a strong wakefield. Unprecedented 1 GeV bunches with 2.5% energy spread were generated by LWFA when the drive laser pulse was guided in a 33 mm long plasma channel [7]. Stability and reproducibility of the acceleration process was later improved considerably by employing a second counter propagating laser pulse [8]. Here, the second pulse injects some plasma electrons into the accelerating phase of the laser wakefield excited by the first pulse. According to measurements and supporting numerical simulations, the accelerated bunches have a typical duration of the order or less than 10 fs, energies of tens to hundreds of MeVs, a root-mean-square (rms) energy spread of a few per cent, and a charge of tens to hundreds of pC. These parameters make femtosecond relativistic electron-bunches a qualitatively new object and a new tool in physical research, mainly due to the small size of bunches compared to a bunch from a conventional RF accelerator.

Besides the strong accelerating field, there is also a strong focusing field in the wakefield, so that electrons are oscillating around the wakefield axis while being accelerated. Such an electron motion, called betatron oscillation, leads to the generation of electromagnetic radiation such as in a conventional undulator. Femtosecond x-ray pulses from electrons accelerating in a laser wakefield were observed in experiments [9]–[12]. Such pulses are interesting for a number of applications, e.g. for studying ultra-fast physical, chemical and biological processes. Recently, visible synchrotron radiation was observed when $\sim$60 MeV fs electron bunches from an LWFA were sent through a conventional undulator [13]. However, the situation in LFWA differs from that in an undulator or a synchrotron radiation source in many aspects. First of all, the energy of an electron undergoes considerable change in LWFA (the electron is accelerated). This, along with changes in the accelerating and focusing field, leads to significant changes in the wavelength and amplitude of the betatron oscillations while the particle is accelerated. Moreover, electrons in the bunch show different betatron amplitudes r_0 (and therefore different betatron strength parameter $K = 2\pi\gamma r_0/\lambda_b$, where γ is the relativistic factor and λ_b is the betatron wavelength [14]), ranging from zero to some maximum value comparable to the bunch radius. Furthermore, in spite of the fs bunch duration, the spread in the betatron frequencies due to the finite bunch length leads to fast betatron phase mixing and bunch decoherence in LWFA [15]. Such bunch dynamics means, particularly, that the conventional approach to calculate the radiated field by the use of the bunch form factor [16] may fail in the case of LWFA.

Radiation from a single electron, in the case of a large betatron strength parameter ($K \gg 1$, wiggler limit), was calculated assuming broadband synchrotron emission [9, 12], [17]–[19]. In this paper, we study, for the first time, spectral and angular distribution of coherent and incoherent electromagnetic radiation emitted by an fs electron bunch during acceleration in a channel-guided LWFA. Our simulations are based on exact expressions derived from Lienard–Wiechert potentials and make no assumptions. The simulations show that the radiation in the coherent range of frequencies reveal details of the acceleration process and properties of the electron bunch, such as its duration, charge, energy and offset (if present) with respect to the wakefield axis. The incoherent range of the spectrum, which extends to the x-ray frequency range, consists of rather broad peaks caused by the acceleration. Details of the simulations as well as laser and e-bunch dynamics in channel-guided LWFA are described in the next section. In sections 3 and 4, results on emission in, respectively, coherent and incoherent ranges of the spectrum are presented. In section 5, the radiated energy, power and the pulse duration are estimated. In the last section, we summarize the results.

2. The parameters, the model, electron bunch and laser pulse dynamics

First, we specify the parameters of the problem choosing values typical for channel-guided LWFA. For definiteness, we consider an axially symmetrical Gaussian laser pulse with wavelength of 800 nm, spot radius $w_0 = 39.8\,\mu$m, a full-width-at-half-maximum (FWHM) duration of 62.5 fs, and a normalized peak amplitude [2] of $a_0 = 0.7$; the laser pulse is linearly polarized. These parameters correspond to a peak intensity of $\approx 10^{18}\,\mathrm{W\,cm^{-2}}$. We further assume a 43.77 mm long plasma channel, with an on-axis electron concentration of $4.52 \times 10^{17}\,\mathrm{cm^{-3}}$ (plasma wavelength $\lambda_p = 50\,\mu$m), in which the laser pulse generates a wakefield. The channel radius was chosen to be somewhat larger than the matched value w_0, namely, $r_{ch} = 44.8\,\mu$m. This was done to minimize the oscillations in the peak laser intensity and in the wakefield amplitude. These oscillations are caused by the finite laser power [20]. For the laser pulse parameters under consideration, the peak power in the pulse (which is 26 TW), normalized to the critical power for self-focusing [20], is 0.38; the pulse contains 1.74 J energy. The amplitude of the accelerating component of the wakefield is $11\,\mathrm{GV\,m^{-1}}$ at the entrance of the plasma channel. The laser pulse dynamics and the laser wakefield generated by the pulse are simulated with the fully relativistic particle code WAKE [21, 22]. The normalized peak intensity, as function of the propagation distance in the channel, is plotted in figure 1. We assume that an electron bunch is formed via some internal or external injection mechanism in the plasma channel or is injected in it. The electron bunch to be accelerated in the channel is modelled by an initially random Gaussian distribution of positions and momenta of test particles. Initially, the bunch has a relativistic factor $\gamma_0 = 200$ (energy of 102.2 MeV), FWHM transverse (x and y) sizes of 3.75 μm, an FWHM duration of 6.25 fs (corresponding to an FWFM bunch length of $\approx 1.88\,\mu$m), the normalized transverse emittances of 0.8 μm, and an rms energy spread of 3%. 10^4 test particles were used in our simulations, unless specified otherwise.

Let us now look at the features of electron motion in LWFA. The transverse position, x, of an electron in a laser wakefield is described by the expression [15]

$$x = x_0(\varphi_{b0}/\varphi_b)^{1/2}\cos(\varphi_b - \varphi_{b0}), \tag{1}$$

where $\varphi_b = 2(f\gamma/E_z^2)^{1/2}$ is the betatron phase, γ is the relativistic factor, E_z and f are the normalized accelerating field and gradient of the focusing field, respectively, the subscript '0'

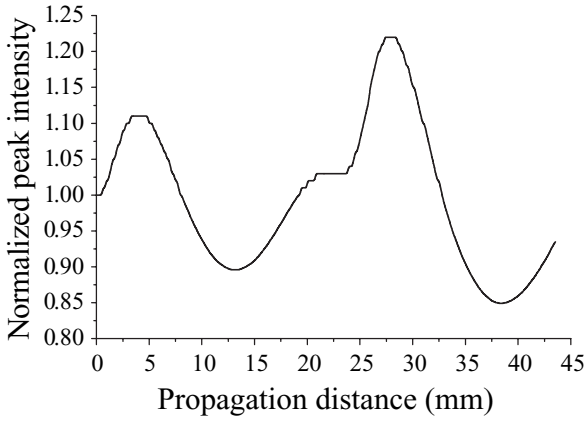

Figure 1. The maximum laser pulse intensity, normalized to its initial value, as a function of the propagation distance in the plasma channel.

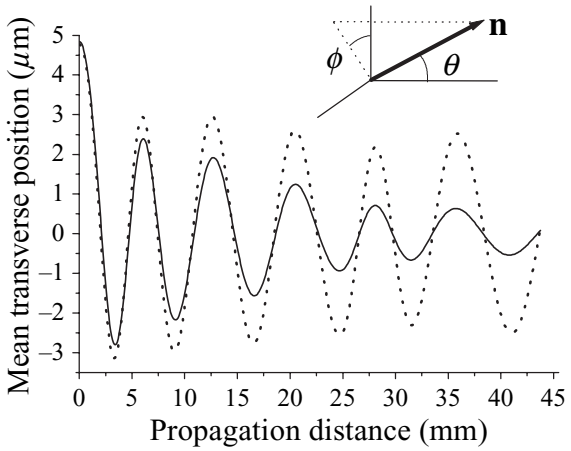

Figure 2. Trajectory of an electron in LWFA (dotted curve). Initially $\gamma_0 = 200$. The solid curve shows the mean transverse position of a bunch of electrons with the same initial energy and offset of 4.77 μm. During acceleration, the bunch shows betatron oscillations quickly damped due to the betatron phase mixing. In both cases, finally, $\gamma_m \approx 1000$. Plasma channel length is 43.77 mm. The vector **n** is directed towards the observer, θ is the observation (polar) angle, ϕ is the azimuthal angle.

denotes the initial values. In LWFA, the betatron phase φ_b and betatron frequency $\omega_b = d\varphi_b/dt = \omega_p(f/\gamma)^{1/2}$ (here ω_p is the plasma frequency) [15, 23] change in time due to the varying energy of the particle and the laser wakefield seen by the electron. An example of a simulated electron trajectory (see figure 2, dotted curve) shows that the betatron wavelength grows during acceleration in LWFA, in agreement with (1). In the case of an electron bunch, despite the fact that the bunch is much shorter than the plasma wavelength, the betatron frequency becomes dependent on the longitudinal position in the bunch, so that electrons in the bunch end up with different betatron phases after acceleration. This leads to betatron phase mixing in the case of on-axis propagation of the bunch: the accelerated bunch radius becomes

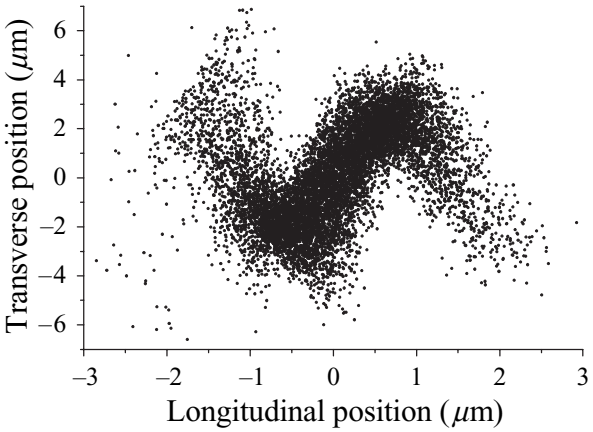

Figure 3. Spatial distribution of electrons in the accelerated bunch. The simulation parameters are the same as in figure 2 (solid curve).

dependent on the longitudinal position [15]. When an fs bunch is injected off-axis, fast damping of the betatron oscillations performed by the bunch compared to that of a single particle (see figure 2), is an indication of such betatron phase mixing and accompanied bunch decoherence, as described in [15]. In figure 3, we show the electron distribution in the accelerated bunch, which is typical for off-axis propagation of the bunch.

3. Coherent radiation

The electromagnetic radiation from a bunch of electrons, in the far field, can be calculated from the spatial motion of the electrons using the Lienard–Wiechert potentials, as given in [24]:

$$W_{\omega,\Omega} = A \left| \int_0^{t_m} \sum_{j=1}^{N_e} \frac{\mathbf{n} \times [(\mathbf{n} - \boldsymbol{\beta}_j) \times \mathbf{a}_j]}{(1 - \mathbf{n}\boldsymbol{\beta}_j)^2} \, \mathrm{e}^{\mathrm{i}\omega(t - \mathbf{n}\mathbf{r}_j/c)} \, \mathrm{d}t \right|^2 . \tag{2}$$

Here $W_{\omega,\Omega} = \mathrm{d}^2 W/\mathrm{d}\omega \, \mathrm{d}\Omega$ is the energy radiated in a unit solid angle, Ω at frequency ω, $A = e^2/4\pi^2 c \approx 1.95 \times 10^{-38}$ J s; $\mathbf{n}$ is a unit vector directed to the observation point and is determined by the spherical polar, θ (observation angle), and azimuthal, ϕ, angles as depicted in figure 2. $\mathbf{r}_j$ is the position of jth electron, $\boldsymbol{\beta}_j = \mathrm{d}\mathbf{r}_j/\mathrm{d}(ct)$ and $\mathbf{a}_j = \mathrm{d}\boldsymbol{\beta}_j/\mathrm{d}t$ are the velocity and acceleration normalized to the speed of light, N_e is the number of particles in the bunch. The acceleration of the electrons in LWFA is considered over a time interval $[0, t_m]$. To calculate the radiated energy (2) one needs to know the evolution of the position, $\mathbf{r}_j(t)$, of each particle in time. The laser pulse dynamics and the laser wakefield generated by it were calculated by the WAKE code. The electron bunch dynamics in the wakefield were simulated by a particle tracking code. Then, the radiated field was calculated numerically from (2). For our simulations, we have used parameters of the problem specified in the previous section. The electron distribution in the bunch is initially centred at the maximum accelerating field in the first accelerating bucket behind the laser pulse. We also assume that the bunch charge is below the beam-loading limit (see, e.g. [25]) that is the effects of space charge and the plasma wakefield from the bunch are neglected. Accuracy of the numerical results was controlled by choosing sufficiently small calculation steps and a sufficiently large number of test particles.

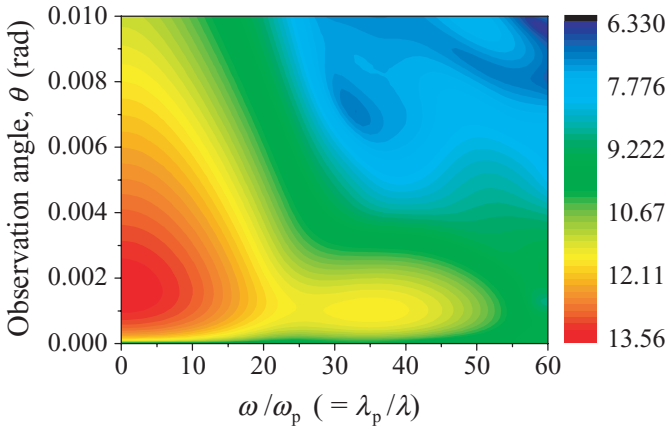

Figure 4. Coherent radiation emitted by an e-bunch in the case of on-axis propagation in LWFA. The spectral and angular distribution of normalized radiated energy, given on a logarithmic scale (specifically, $\lg(W_{\omega,\Omega}/A)$ (see expression (2)) is plotted in figures 4–8) is colour-encoded. The parameters of the bunch are: FWHM transverse (x and y) sizes of 3.75 μm, FWHM duration of 6.25 fs, $\gamma_0 = 200$, rms energy spread of 3%, the normalized transverse emittances of 0.8 μm. 10^4 test electrons are used in the simulation.

Particularly, the number of test particles N_λ, which have a coordinate in the emission direction (which is in fact the bunch propagation direction because of the small observation angles (see below)) within a spatial interval equal to the radiated wavelength λ, should be much larger than unity, that is $N_\lambda \sim N_b\lambda/l_b \gg 1$, where l_b and N_b are length of the bunch and number of test particles in it, respectively. More details on simulation of bunch dynamics as well as properties of the generated laser wakefield can be found in [15] and references therein.

Figure 4 shows the radiated energy normalized to A, in the logarithmic scale, namely, $\lg(W_{\omega,\Omega}/A)$. In this case the bunch propagates along the wakefield axis (zero offset) and reaches an energy of 513 MeV after acceleration in the plasma channel. Strong emission at wavelengths comparable to or longer than the bunch length can be seen. We found that in this range of wavelengths the radiated energy scales as $\sim N_e^2$, which shows that the radiation is coherent. Note that during acceleration the bunch length is conserved with high accuracy [15]. It can further be seen that the radiated energy possesses minimum on axis ($\theta = 0$) and is confined to small observation angles of the order of $1/\gamma$. The distribution of the radiation does not depend on the azimuthal angle due to the axial symmetry of the electron distribution. In the case of fs e-bunches accelerated in LWFA, the coherent radiation corresponds to the infrared range. It should be noted that, as it is well known, the radiation at frequencies below ω_p is damped in plasmas. In figure 5, we have plotted the radiation in the coherent range at an observation angle of 1.5 mrad for three different bunch lengths. The results show that the shorter the bunch, the broader the coherent range. At low frequencies, when $W_{\omega,\Omega}$ decreases monotonically, the radiated energy scales approximately as $\exp[-(\omega\sigma/c)^2]$ (here σ is the rms bunch length) that agrees with the form factor formalism [16]. This fact can be used to experimentally determine the fs bunch duration, measurement of which is an experimental challenge.

Suppose now that the bunch propagates in LWFA off-axis (off-axis propagation may take place both in single- and multi-stage LWFA [15]) and has an initial transverse offset of 4.77 μm.

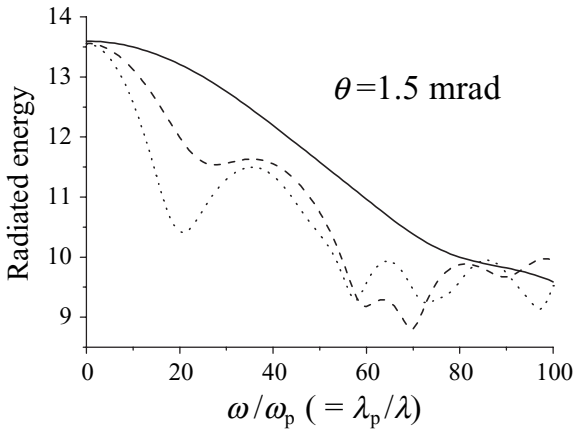

Figure 5. Spectrum of the coherent radiation, in the case of on-axis propagation of the bunch, plotted for different FWHM bunch lengths: 0.94 μm (solid curve), 1.88 μm (dashed curve; this case corresponds to parameters of figure 4), and 2.88 μm (dotted curve).

This case corresponds to the solid line in figure 2. Keeping other parameters the same as in figure 4, we have calculated the radiated energy distribution. The result is plotted in figure 6. We see clear differences between the radiation from off-axis bunch propagation compared to that from on-axis propagation (compare figures 4 and 6). In particular, the coherent range extends to shorter radiated wavelengths; the radiated energy becomes dependent on the azimuthal angle. Moreover, there is a gap at certain observation angles in the case of $\phi = 0$. In addition, there is a strong on-axis radiation. These features allow on- and off-axis bunch propagation in LWFA to be experimentally distinguished.

For the sake of better understanding of the features of the coherent radiation found in the simulations, we rewrite expression (2) in the form

$$W_{\omega,\Omega} = A \left| \sum_{j=1}^{N_e} \left[\mathbf{D}_j(t_m) - \mathbf{D}_j(t_0) - \mathrm{i}\omega \int_0^{t_m} \mathbf{B}_j \mathrm{e}^{\mathrm{i}\omega(t - \mathbf{n}\mathbf{r}_j/c)}\, \mathrm{d}t \right] \right|^2, \tag{3}$$

where $\mathbf{B}_j = \mathbf{n} \times [\mathbf{n} \times \boldsymbol{\beta}_j]$, $\mathbf{D}_j(t) = [\mathbf{B}_j/(1 - \mathbf{n}\boldsymbol{\beta}_j)] \exp[\mathrm{i}\omega(\mathrm{t} - \mathbf{n}\mathbf{r}_j/c)]$. Then, taking into account that $\beta_x, \theta \ll 1$ and $\gamma_m^2 \gg \gamma_0^2$, estimating the integral in (3) using (1), we have found that in the coherent range of frequencies

$$W_{\omega,\Omega} \approx A \left| \sum_{j=1}^{N_e} \mathbf{D}_j(t_m) \right|^2, \tag{4}$$

so that the radiation in the coherent range is determined by the final parameters of the accelerated electrons. The comparison of the coherent radiation, simulated using expressions (2) and (4), indeed showed a good agreement between the two results, for both on- and off-axis bunch propagation. This shows that the **D**-terms in (3), which are typically neglected, for example, in conventional undulator theory, play a crucial role in the case of LWFA due to acceleration. More details can be revealed in the case of a single electron. In this case $|\mathbf{D}_m|^2 \approx 4\gamma_m^4 \mathbf{B}_m^2/(1 + \gamma_m^2 \mathbf{B}_m^2)^2$, where $\mathbf{B}_m^2 \approx \theta^2 - 2\theta\alpha\cos(\phi) + \alpha^2$ and $\alpha \equiv \beta_{x,m}$ is the angle, with respect to the propagation

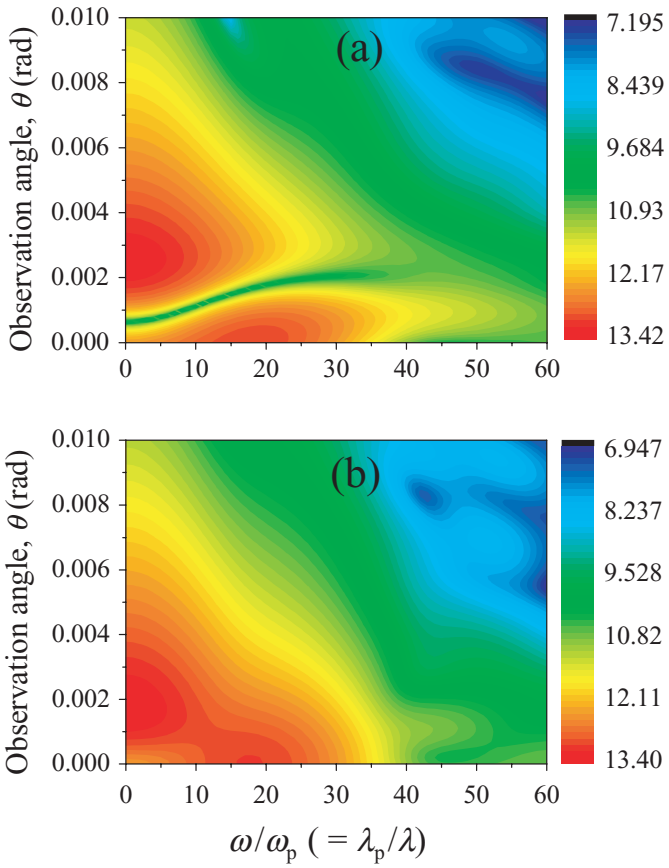

Figure 6. Coherent radiation from a bunch injected off-axis, shown for azimuthal angles $\phi = 0$ (a) and $\phi = \pi/2$ (b). The bunch parameters are the same as in figure 4 except the initial offset of 4.77 μm. The evolution of the mean transverse position of the bunch is shown in figure 2 (solid line).

axis, z, with which the electron exits the wakefield (here the values with subscript m are taken at time moment t_m, i.e. at the end of acceleration process). One can see that the value of $|\mathbf{D}_m|^2$ has a minimum at an observation angle $\theta_* = \alpha\cos(\phi)$. There are also maxima at $\theta_{1,2} = \theta_* \pm [\gamma_m^{-2} - \alpha^2\sin^2(\phi)]^{1/2}$ (remember, however, that $\theta \geqslant 0$), at which $|\mathbf{D}_m|^2 \approx \gamma_m^2$. Note also that $W_{\omega,\Omega}$ does not depend on ω in the case of a single electron. These findings agree well with simulations for a single electron, and they reasonably agree with the simulations for an electron bunch. In the case of a bunch propagating off-axis, the observation angle θ_*, at which the minimum is reached, becomes dependent on the frequency, as can be seen in figure 6(a). The difference between spectra of a bunch and an electron, for off-axis propagation, is caused by the following dynamics of the e-bunch in the wakefield. The bunch does not maintain its shape during acceleration as discussed in section 2 (see also [15]). The shorter the bunch compared to the plasma wavelength, the weaker the phase mixing process and the higher the similarity of the coherent radiation distribution for an entire bunch, compared to that for a single electron. Thus, the coherent radiation from an LWFA is determined mainly by the final parameters of the bunch and gives valuable information on its properties and dynamics. These are fs bunch length, the number of electrons in the bunch, the offset and transverse velocity of the accelerated bunch

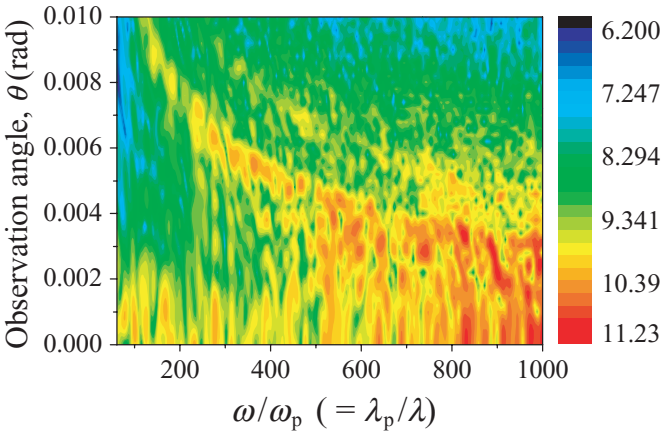

Figure 7. The distribution of incoherent radiation from a channel-guided LWFA. The bunch parameters are the same as those used in figure 4.

at the exit of plasma, the bunch dynamics during acceleration (betatron phase mixing), and the final energy of the bunch. Therefore, an observation of the radiation can provide a valuable, non-destructive diagnostic method for LWFA.

4. Incoherent range of frequencies

In this section, the results of simulations in the range of higher frequencies, where the emission is incoherent, i.e. where we found that the radiated energy scales as $\sim N_e$, are presented. In figure 7, the spectral and angular distribution of the radiation for the same parameters as we used for figure 4 is shown. Here, the spectrum of the emitted radiation extends to a wavelength of 50 nm. Details of the distribution of the radiation, which is typical for channel-guided LWFA, can be seen. Particularly, the spectrum consists of rather broad peaks. The radiation is again well collimated. For comparison, the spectrum from a conventional undulator is peaked at frequencies given by $\omega_n = 2n\gamma^2(2\pi c/\lambda_u)/[1 + K^2/2 + (\gamma\theta)^2]$, where λ_u is the undulator period and n is the harmonic order (see, e.g. [26]). The width of the peaks are given by the natural spectral width $\delta\omega_n/\omega_n = 1/(nN_u)$, where N_u is the number of undulator periods, and the energy spread in the bunch. In contrast, according to our simulations, the large width of the peaks in the spectrum emitted from an LWFA can be attributed mainly to the large change in the energy of electrons during acceleration, but also to the relatively small number of transverse oscillations performed by electrons, corresponding to $N_u \approx 6$ in our simulations (see figure 2). The maximum betatron strength parameter K of the accelerated electrons is of the order of unity. The radiation was found to be not sensitive to an energy spread of a few per cent because during acceleration the energy of each electron changes in a quite broad range.

Using the same parameters as in figures 4 and 7, we have calculated the radiation for even higher frequencies extending to x-ray range, namely up to $\omega = 5 \times 10^4\omega_p$, which corresponds to a wavelength of 1 nm. To calculate the radiated energy correctly, for this simulation 3×10^4 test particles were used to make sure that the distance between them is much shorter than the radiation wavelength. The result is shown in figure 8. The distribution of the radiated energy is qualitatively the same as in figure 7. Figure 8 is less detailed, but now the overall behaviour of the distribution can be clearly seen. The radiated energy, W, grows with frequency and,

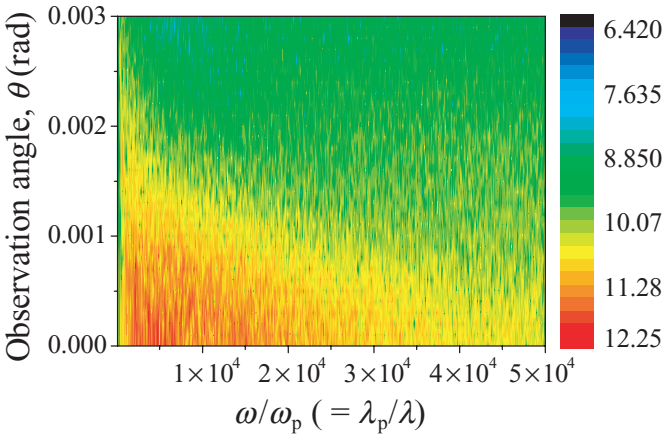

Figure 8. Incoherent radiation: down to 1 nm wavelength. Simulation parameters are the same as in figures 4 and 7. 3×10^4 test particles were used for this simulation.

after reaching some frequency, $\omega_c \sim 5 \times 10^3 \omega_p$, the energy decreases globally. This agrees with the estimation based on the synchrotron radiation theory $\omega_c \sim (3/2)\gamma^3 r_0 \omega_b^2/c$ [19], if one substitutes here final parameters of the accelerated electrons. In the case of off-axis propagation of the bunch, for an arbitrary azimuthal angle, simulations showed that the distribution of the radiation looks pretty much the same as in the case of on-axis propagation.

5. Radiated energy, power and the pulse length

The radiation emitted by a single electron, for the case presented in figure 2 (dotted line), was also simulated. The distribution of the radiation in the incoherent range of frequencies was found to be qualitatively the same as that for an electron bunch. Integrating the expression for $dW/d\Omega$ (see [24]) numerically, we found that a total energy of $W \approx 10^{-18}$ J is emitted by the electron, which is negligible compared to electron's final energy of 8.2×10^{-11} J. This justifies the neglect of the radiation reaction force in our simulations. About half of the radiated energy is emitted during the last 20% of the acceleration distance. We also found that for the laser and plasma parameters we have used $W \sim x_0^2$, x_0 being the initial betatron amplitude. Taking into account these results, we have estimated that, for bunch parameters used in figures 7 and 8 (on-axis propagation), $\sim 10^{-19}\, N_e$ J energy is emitted in the incoherent range of frequencies. For example, when $N_e = 5 \times 10^8$, which corresponds to 80 pC charge, the bunch radiates $W_b^{(i)} \sim 5 \times 10^{-11}$ J energy in the incoherent range. The energy emitted in the coherent range of frequencies can be estimated from the following expression: $W_b^{(c)} \sim N_e^2 W_1$, where W_1 is the energy emitted by a single electron. According to the results of section 3, one has $W_1 \sim A(\mathbf{D}_m^2)_{\max} \Delta\omega \Delta\Omega$. Taking into account that $(\mathbf{D}_m^2)_{\max} \approx \gamma_m^2$, $\Delta\omega \sim c/l_b$, where l_b is the rms bunch length, and $\Delta\Omega \sim \pi\theta^2 \sim \pi/\gamma_m^2$, we can write

$$W_b^{(c)} \sim \pi A N_e^2 c/l_b. \tag{5}$$

For example, when $l_b = 0.8\,\mu$m (corresponding FWHM bunch duration is 6.25 fs) and $N_e = 5 \times 10^8$, we find that $W_b^{(c)} \sim 6 \times 10^{-6}$ J. Comparing this with the energy radiated in the

incoherent range, $W_b^{(i)}$, one concludes that the energy emitted in the coherent range gives a major contribution to the total energy emitted by LWFA.

The power radiated by an electron is [24]

$$P_{\rm rad} = \left(\frac{2e^2}{3c}\right)\left[\gamma^4\left(\frac{{\rm d}\boldsymbol{\beta}}{{\rm d}t}\right)^2 + \gamma^6\left(\boldsymbol{\beta}\frac{{\rm d}\boldsymbol{\beta}}{{\rm d}t}\right)^2\right]. \tag{6}$$

One can see that the longitudinal component of the electron's acceleration can be typically neglected since it is proportional to $1/\gamma^3$ (see, e.g. [27]). Then, we find that in LWFA

$$P_{\rm rad} = \left(\frac{2e^2}{3c}\right)\gamma^4(k_{\rm b}x)^2\left[1+(\gamma k_{\rm b}x)^2\tan^2(\varphi_{\rm b}-\varphi_{\rm b0})\right], \tag{7}$$

where $k_{\rm b} = \omega_{\rm b}/c$ is the betatron wavenumber and x is given by expression (1). The first and second terms in (7) are proportional to $x_0^2\gamma^{3/2}$ and $x_0^4\gamma^2$, respectively. The energy gain of the electron in the wakefield is ${\rm d}(m_{\rm e}c^2\gamma)/{\rm d}t = ce|E_z|$ [27], where E_z is the accelerating field. Comparing this expression with (7), for parameters typical for LWFA, one sees that the radiated power becomes comparable to the energy gain only when the energy of an electron reaches the TeV range (i.e. for $\gamma \sim 10^{12}$ and larger).

The length of the electromagnetic pulse emitted by an LWFA is determined by the longitudinal slippage between the electron bunch and the radiation and can be estimated from $l_{\rm EM} \sim |\beta_{\rm b} - \beta_{\rm g}|L_{\rm pr}$. Here $L_{\rm pr}$ is the bunch propagation distance, $\beta_{\rm b} = v_{\rm b}/c$ and $\beta_{\rm g} = v_{\rm g}/c = [1-(\omega_{\rm p}/\omega)^2]^{1/2}$ are the bunch velocity and the group velocity of the radiation at frequency ω; both velocities are normalized to the speed of light. If one considers frequencies $\omega/\omega_{\rm p} > (\gamma^{-2} + 2l_{\rm b}/L_{\rm pr})^{-1/2}$ (when, for example, lower frequencies are filtered out; for typical parameters of the problem, this condition corresponds to $\omega/\omega_{\rm p} > 100$), the emitted pulse length is of the order of the bunch length, $l_{\rm EM} \sim l_{\rm b}$, that corresponds to the pulse duration of the order of 10 fs. When lower frequencies are included into consideration, taking into account that most of the energy is emitted in the coherent range, where $\omega/\omega_{\rm p} < c/(\omega_{\rm p}l_{\rm b})$, the pulse length can be roughly estimated from $l_{\rm EM} \sim (\omega_{\rm p}l_{\rm b}/c)^2 L_{\rm pr}$.

6. Summary

In conclusion, we have calculated electromagnetic radiation from a channel guided LWFA, based on exact expressions derived from Lienard–Wiechert potentials. The results show that LWFA is a source of a well-collimated electromagnetic radiation with specific features of the spectral and angular distribution. Particularly, broadband coherent radiation is emitted at wavelengths comparable to or longer than the bunch length. This radiation typically lies in the infrared range. The energy is emitted predominantly in the coherent range. It is found that the angular distribution and spectrum of the coherent radiation is mainly determined by the final parameters of an accelerated bunch and contains information on length, energy, charge and offset of the bunch. Correspondingly, the radiation from LWFA can be used as a diagnostic tool. The spectrum of the emitted electromagnetic pulse extends towards the x-ray frequency range. In the incoherent range of the spectrum, the spectrum consists of rather broad peaks; the radiation remains well collimated, as in synchrotron radiation sources and free electron lasers.

Acknowledgments

This work has been supported by the Dutch Foundation for Fundamental Research on Matter (FOM) under the 'Laser wakefield Accelerators' program, by the Dutch Ministry of Education, Culture and Science (OC&W), and by the European Community—New and Emerging Science and Technology Activity under the FP6 'Structuring the European Area' program (project EuroLEAP, contract number 028514). We acknowledge Professor Patrick Mora (CPHT, École Polytechnique, Palaiseau, France) for providing the WAKE code and detailed explanations on it.

References

[1] Tajima T and Dawson J M 1979 *Phys. Rev. Lett.* **43** 267
[2] Esarey E, Sprangle P, Krall J and Ting A 1996 *IEEE Trans. Plasma Sci.* **24** 252
[3] Kotaki H, Kando M, Oketa T, Masuda S, Koga J K, Kondo S, Kanazawa S, Yokoyama T, Matoba T and Nakajima K 2002 *Phys. Plasmas* **9** 1392
[4] Mangles S P D *et al* 2004 *Nature* **431** 535
[5] Geddes C G R, Toth Cs, van Tilborg J, Esarey E, Schroeder C B, Bruhwiler D, Nieter C, Cary J and Leemans W P 2004 *Nature* **431** 538
[6] Faure J, Glinec Y, Pukhov A, Kiselev S, Gordienko S, Lefebvre E, Rousseau J-P, Burgy F and Malka V 2004 *Nature* **431** 541
[7] Leemans W P, Nagler B, Gonsalves A J, Toth C, Nakamura K, Geddes C G R, Esarey E, Schroeder C B and Hooker S M 2006 *Nat. Phys.* **2** 696
[8] Faure J, Rechatin C, Norlin A, Lifschitz A, Glinec Y and Malka V 2006 *Nature* **444** 737
[9] Rousse A *et al* 2004 *Phys. Rev. Lett.* **93** 135005
[10] Phuoc K Ta, Corde S, Shah R, Albert F, Fitour R, Rousseau J-P, Burgy F, Mercier B and Rousse A 2006 *Phys. Rev. Lett.* **97** 225002
[11] Phuoc K Ta *et al* 2007 *Phys. Plasmas* **14** 080701
[12] Kneip S *et al* 2008 *Phys. Rev. Lett.* **100** 105006
[13] Schlenvoigt H-P *et al* 2008 *Nat. Phys.* **4** 130
[14] Michel P, Schroeder C B, Shadwick B A, Esarey E and Leemans W P 2006 *Phys. Rev.* E **74** 026501
[15] Khachatryan A G, Irman A, van Goor F A and Boller K-J 2007 *Phys. Rev. ST Accel. Beams* **10** 121301
[16] Nodvick J S and Saxon D S 1954 *Phys. Rev.* **96** 180
[17] Kostyukov I, Kiselev S and Pukhov A 2003 *Phys. Plasmas* **10** 4818
[18] Kiselev S, Pukhov A and Kostyukov I 2004 *Phys. Rev. Lett.* **93** 135004
[19] Phuoc K Ta, Burgy F, Rousseau J-P, Malka V, Rousse A, Shah R, Umstadter D, Pukhov A and Kiselev S 2005 *Phys. Plasmas* **12** 023101
[20] Esarey E, Sprangle P, Krall J and Ting A 1997 *IEEE J. Quantum Electron.* **33** 1879
[21] Antonsen T M Jr and Mora P 1992 *Phys. Rev. Lett.* **69** 2204
[22] Mora P and Antonsen T M J 1996 *Phys. Rev.* E **53** R2068
[23] Esarey E, Shadwick B A, Catravas P and Leemans W P 2002 *Phys. Rev.* E **65** 056505
[24] Jackson J D 1975 *Classical Electrodynamics* 2nd edn (New York: Wiley) chapter 14
[25] Khachatryan A G, van Goor F A, Boller K-J, Reitsma A J W and Jaroszynski D A 2004 *Phys. Rev. ST Accel. Beams* **7** 121301
[26] Freund H P and Antonsen T M Jr 1996 *Principles of Free-Electron Lasers* (London: Chapman and Hall)
[27] Khachatryan A G 2002 *Phys. Rev.* E **65** 046504